# Reconstruction of Photon Conversions and Precise Measurement of Photon Energy at BESⅡ *

ZHANG Chang-Chun[1,2;1)] WANG Zhe[3] YUAN Ye[1]

1 (Institute of High Energy Physics, CAS, Beijing 100049, China)
2 (Department of Technical Physics, Peking University, Beijing 100871, China)
3 (Department of Engineering Physics, Tsinghua University, Beijing 100084, China)

**Abstract** Using Monte Carlo simulation, reconstruction of photon conversions is studied, and the detection efficiency and energy resolution as a function of photon energy are obtained. The d$E$/d$x$ correction for the electrons from photon conversions and the energy scale for the photons are calibrated with BESⅡ data. An improved Crystal Ball function describes well the energy distribution of the photons. Photon energy resolutions in the range from 2.3 to 3.8MeV are found for the photons with energy from 100 to 260MeV at the BESⅡ detector.

**Key words** photon conversion, photon reconstruction, d$E$/d$x$ correction, photon energy resolution, BESⅡ detector

## 1 Introduction

Precise measurement of photon energy, specially for low energy photons, is an important issue in high energy physics experiments. Photons produced in the $J/\psi \to \gamma\eta_c(1S)$ and $\psi(2S) \to \gamma\chi_{cJ}$ ($J = 0,1,2$) radiative decays carry an energy from 115 to 261MeV. The CsI(Tl) crystal calorimeter at CLEO provides an energy resolution of 4.8MeV for 100MeV energy photon[1]. However, energy resolution in a calorimeter consisting of proportional wire chamber or self-quenching streamer tubes is much worse. It is interesting to explore a new method for photon energy measurement with an improved energy resolution at the BESⅡ detector[2].

We have employed the photon conversion technology in photon energy measurement. Each photon is reconstructed from its converted $e^+e^-$ pair. Energy resolutions in the range from 2.3 to 3.8MeV are determined for the photons with energy from 100 to 260MeV using GEANT3 based Monte Carlo (MC) simulation package SIMBES[3]. MC study shows that momentum resolution from 1.6 to 4.1MeV/$c$ in the central part of the momentum distribution can be obtained for electrons carrying momentum as low as 60 to 250MeV/$c$, but a tail appears at the lower side of the distribution. The electrons produced from conversion process of photons with energy from 100 to 260MeV occur just in this low momentum region. Momentum correction due to ionization energy loss (d$E$/d$x$) for the electrons and energy scale for the photons are calibrated using the $J/\psi$ and $\psi(2S)$ data, collected by the BESⅡ detector operating at the BEPC $e^+e^-$ colliding machine.

The BESⅡ, a conventional solenoidal magnet spectrometer, is described elsewhere[4]. A 12-layer vertex chamber (VC) surrounding a beam pipe gives trigger condition. A forty-layer main drift chamber (MDC), located radially outside the VC, provides trajectory and energy loss (d$E$/d$x$) information for

Received 9 September 2005, Revised 29 December 2005
* Supported by National Natural Science Foundation of China (19991480) and Knowledge Innovation Project of CAS (U-503(IHEP))
1) E-mail: zhangcc@ihep.ac.cn

charged tracks over 85% of the total solid angle. The momentum resolution is $\sigma_{\rm P}/p = 0.017\sqrt{1+p^2}$ ($p$ in GeV/$c$), and the d$E$/d$x$ resolution for hadron tracks is $\sim 8\%$. An array of 48 scintillation counters surrounding the MDC measures the time-of-flight (TOF) of charged tracks with a resolution of $\sim$ 200ps for hadrons. Outside the TOF system is a lead-gas barrel shower counter (BSC), which has 12 radiation length and covers about $\sim$80% of the total solid angle with an energy resolution of $\sigma_{\rm E}/E = 22\%/\sqrt{E}$ ($E$ in GeV). The solenoidal coil supplies a 0.4T magnetic field over the tracking volume.

## 2 Photon reconstruction

The process of photon conversion to $\rm e^+e^-$ pair happens along the way from the beam line to the inside of the MDC. It is expected that the observed conversion rate of photons is peaked in a beam pipe region, where the beam pipe, outer wall of the VC and inner wall of the MDC are located.

It is required to find photon conversion point (CP) with the input parameters of electron tracks calculated at the origin of the detector coordinate system. We choose two tracks with opposite charge and good helix fit. Two circles, as projection of the electron and positron trajectories in the $xy$ plane (the beam line is the $z$ axis), touch at a point in principle for nearly zero opening angle between their outgoing directions. However, the number of crossing points found in photon reconstruction procedure can be one, two or zero due to the uncertainty of the input track parameters. The photon conversion point is calculated from their averaged position (coordinates of two circle centers) if two crossing points are (no crossing point is) found.

The photon conversion length $R_{xy}$ is defined as a distance between $\rm e^+e^-$ interaction point (IP) and the CP. A MC sample for the $\psi(2S) \to \gamma\chi_{c0}$ decay is generated with zero widths of both $\psi(2S)$ and $\chi_{c0}$ states, where the photons are emitted with an unique energy of 260.7MeV. Comparisons between kinematics in MC generation and output from the photon reconstruction for $R_{xy}$, $\phi_{R_{xy}}$, and $z$ position of electrons at the CP are shown in Fig. 1. Here, $\phi_{R_{xy}}$ is the azimuthal angle of the vector $R_{xy}$. Resolutions in $R_{xy}$, $\phi_{R_{xy}}$, and $z$ position of electrons at the CP are determined to be $\sigma_{R_{xy}} = 1.3\pm0.1$cm, $\sigma_{\phi_{R_{xy}}} = 0.57^\circ\pm0.03^\circ$, and $\sigma_{z_e} = 1.6\pm0.1$cm in the central region of their distributions. The uncertainty in the $R_{xy}$ determination is mainly caused by a small opening angle between outgoing directions of electron and positron, and may become larger for photons with higher energy. Two-dimension scatter plots for the CP distribution in the $xy$ plane at the beam pipe are shown in Fig. 2 for the MC generated and reconstructed photons, respectively.

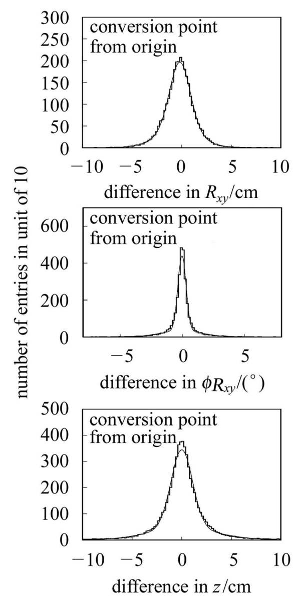


Fig. 1. Difference in $R_{xy}$ (upper), $\phi_{R_{xy}}$ (middle) and $z$ position of electrons (down) at the CP between the MC generation and photon reconstruction. The histograms are the observation, and the solid lines are the fit to double Gaussian function.

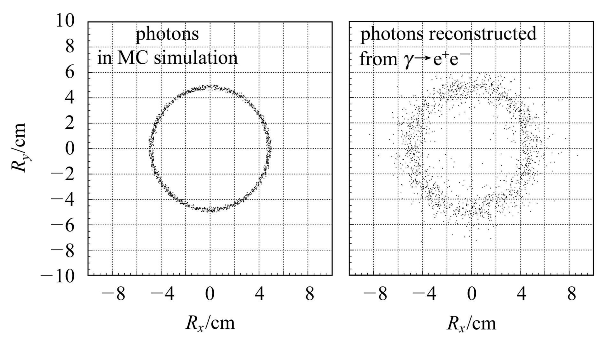


Fig. 2. Scatter plots for the CP distribution in the $xy$ plane are shown for MC generated (left) and reconstructed (right) photons. Round shape for the beam pipe is clearly seen.

Charged tracks in the MDC are reconstructed under an assumption that each track is originally produced at the beam crossing line, and that their momentums are calculated at the closest point of orbit to the beam line. Therefore the outgoing directions of the electron and positron produced at the CP, as well as the momentum of the electrons to that point, need to be recalculated. The difference in the momentum $p_{e^\pm}$ and its direction $\phi_{p_{e^\pm}}$ and $\theta_{p_{e^\pm}}$ for the electrons at the origin between MC generation and MDC tracking before the photon reconstruction are shown in Fig. 3. Wide spread in the distribution of the difference $\Delta\phi_{p_{e^\pm}}$ shows that it is necessary to swim electron momentum from the origin to the CP. Comparisons for the differences in the photon momentum $p_\gamma$ and its direction $\phi_{p_\gamma}$ and $\theta_{p_\gamma}$ at the CP between the MC generation and photon reconstruction are also made using the MC events, and good agreement is reached (see Fig. 4). The invariant mass of $e^+e^-$ pairs and cosine of the opening angle between the vector $R_{xy}$ and photon momentum after the photon reconstruction are shown in Fig. 5 for the MC events of $\psi(2S)\rightarrow\gamma\chi_{c0}$.

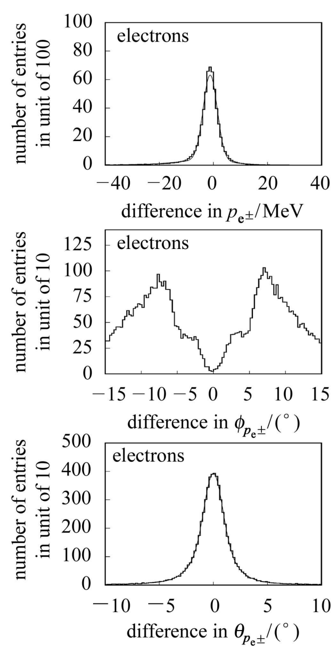


Fig. 3. Difference in $p_{e^\pm}$ (upper), $\phi_{p_{e^\pm}}$ (middle) and $\theta_{p_{e^\pm}}$ (down) of electrons at the origin between the MC generator and MDC tracking before photon reconstruction. The histograms are the observation, and the solid lines are the fit to double Gaussian function.

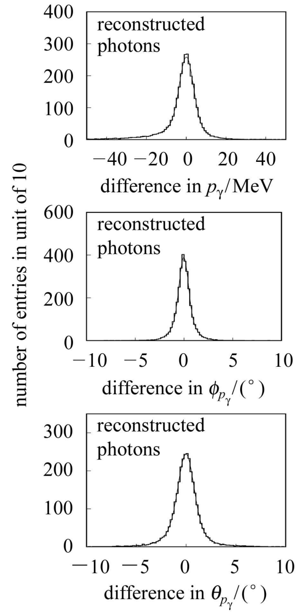


Fig. 4. Difference in $p_\gamma$ (upper), $\phi_{p_\gamma}$ (middle) and $\theta_{p_\gamma}$ (down) of photon momentum between the MC generation and photon reconstruction. The histograms are the observation, and the solid lines are the fit to double Gaussian function.

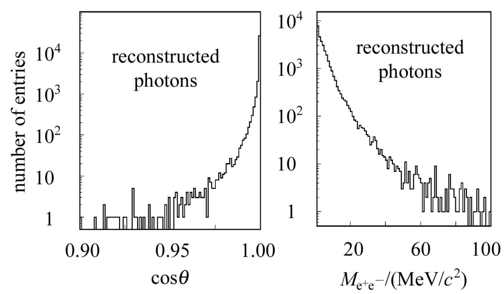


Fig. 5. The invariant mass of $e^+e^-$ pair (right) and cosine of the opening angle between $R_{xy}$ and photon momentum (left).

Electrons converted from photons of interest in physics usually carry low momentum. Because of 0.4T magnetic field and marginal circling of the eletron trajectory in the MDC, the reconstruction efficiency for the electron tracks is low, and tends to be nearly zero when their momentum goes down to a lower limit around 50MeV/$c$. In order to enhance the reconstruction efficiency for photon conversions, it is necessary to apply loose selection criteria in the photon reconstruction.

The region of $R_{xy}<40$cm covers the volumes of the beam pipe, the VC, inner wall of the MDC and first 2—3 layers of the MDC wires. The deflection angle $\theta_{\rm defl}$ between the photon momentum and photon track (a vector from the IP to the CP) should be small. Preliminary requirments on $\cos\theta_{\rm defl}$ and invariant mass of $e^+e^-$ pair (see Fig. 5) are applied in the selection of photon conversion candidates as follows.

1) $R_{xy}<40$cm.

2) $\cos\theta_{\rm defl}<0$ is allowed, if photons are produced within the region of $R_{xy}<0.9$cm near the beam line. Otherwise, requiring that $\cos\theta_{\rm defl}>0$.

3) The invariant mass $M_{e^+e^-}<200{\rm MeV}/c^2$.

The opening angle between the outgoing directions of electron and positron is nearly zero due to zero mass of photon (see Fig. 5), and the observed non-zero of this angle are mostly attributed to the effect of detector resolution. MC study shows that the poor precision in determination of the CP, due to the parallel flying of the electron and positron, is improved for low momentum electrons.

## 3 Photon selection

Further selection of good photon is employed in the analysis procedure. The $Z$ positions of electron and positron trajectories at the CP, $Z_{e^+}$ and $Z_{e^-}$, are calculated, and d$Z$ is defined as the difference of $Z_{e^+}-Z_{e^-}$. It is required that

1) $|{\rm d}Z|<5$cm,

2) the invariant mass $M_{e^+e^-}<20{\rm MeV}/c^2$,

3) $2<R_{xy}<22$cm,

4) the deflection angle $\cos\theta_{\rm defl}>0.9$ and

5) $|\cos\theta|<0.8$, where $\theta$ is the polar angle of the electron track.

Fig. 6 shows the number of good photons in conversion to $e^+e^-$ pair in the BESII detector as a function of $R_{xy}$ for the $\psi(2S)$ hadronic decays in data and MC. To suppress the background from beam-gas and beam-pipe interactions, the total energy $E_{\rm tot}$ and momentum asymmetry $p_{\rm asym}$ in event must satisfy $E_{\rm tot}>E_{\rm beam}/2$ and $p_{\rm asym}<0.9$, respectively. Both the charged and neutral tracks are included in calculation of the total energy. The ratio of vector sum to scalar sum of the momentum for all charged and neutral tracks in the event is defined as the momentum asymmetry. Two peaks at around 0.05m and 0.16m in Fig. 6 correspond to the beam pipe region, and the shape of each peak in data and MC basically agree with each other. The position of the left peak is affected by photon conversions in the VC and slightly shifted from the beam pipe. To assure that $R_{xy}$ is determined correctly in the photon reconstruction, the $R_x$ versus $R_y$ distribution with the VC and the MDC inner wall removed in the MC simulation are drawn in Fig. 2. As one expects, the reconstructed photon conversion points in the $xy$ plane are well scattered around the beam pipe. However, the area of the left peak, where the beam pipe and the VC are located, in the MC is less than that in the data. It shows that the equivalent material for the VC needs to be further improved in the MC simulation. The material parameters for the beam pipe, the VC and the MDC are listed in Table 1[5].

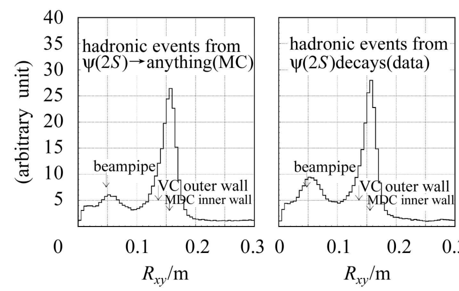


Fig. 6. Number of good photons in conversion to $e^+e^-$ pair in the BESⅡ detector as a function of $R_{xy}$. The photons are selected from hadronic events in the $\psi(2S)$ data (right) and MC (left) sample.

Table 1. The material parameters for the beam pipe, VC and MDC of the BESⅡ detector. Here, $X_0$ is radiation length.

| component | material | radius /cm | thickness /mm | $X/X_0$ (%) |
|---|---|---|---|---|
| beam pipe | Be,Ni,Ti | 4.826 | 1.27 | 0.536 |
| VC outer wall | Al cover carbon fiber | 13.536 | 0.762 | 0.375 |
| VC wires gas | tungsten argon-ethane | | | 0.657 |
| MDC inner wall | aluminum carbon fiber | 15.605 | 2.0 | 1.107 |
| total | | | | 2.675 |

## 4 d$E$/d$x$ correction for electron

Energy loss (d$E$/d$x$) by ionization of atoms is well described by the Bethe-Bloch equation[6], and corrected in the study. In the d$E$/d$x$ correction for charged particles produced near the beam line and traversing the whole beam pipe region, one should take account of the full thickness of materials in the region . However, $e^+e^-$ pairs converted from photons are produced mostly in a region where the VC outer wall and the MDC inner wall are located. Thus the effective thickness of materials between the location, where a pair produced, and the first layer of the MDC wires is required to be estimated in the $\mathrm{d}E/\mathrm{d}x$ correction for each electron or positron track.

A $\mathrm{d}E/\mathrm{d}x$ correction as a function of $R_{xy}$ is required for electrons converted from photons. However, the calculation of $R_{xy}$ needs electron momentum vector as input parameter. Thus, the $\mathrm{d}E/\mathrm{d}x$ correction for the electrons in the study is made with the following steps:

1) Helix fit for charged tracks without $\mathrm{d}E/\mathrm{d}x$ correction;

2) A preliminary $\mathrm{d}E/\mathrm{d}x$ correction using half the full thickness of the materials in the beam pipe region for the fitted electron energy, and followed by reconstruction of photon conversions, determination of $R_{xy}$ and selection of good photons;

3) Final $\mathrm{d}E/\mathrm{d}x$ correction as a function of $R_{xy}$ is estimated with the effective thickness of materials between the CP and first layer of the MDC wires.

Our study shows that the photon energy scale is improved by using the $R_{xy}$-dependent $\mathrm{d}E/\mathrm{d}x$ correction. However, the uncertainty of $R_{xy}$ is dominated by the error of the opening angle between the outgoing directions of electron and positron. Iteration with small $\mathrm{d}E/\mathrm{d}x$ correction, depending on $R_{xy}$ with poor precision, may not improve the result and thus is unnecessary.

A MC sample of $3.8\times10^8$ photons, each carrying 261MeV energy, are generated. The electron momentum difference between measurement and MC generation is shown in the left plot of Fig. 7 for the different $\mathrm{d}E/\mathrm{d}x$ corrections by (a) this study, (b) full thickness of materials in the beam pipe region, and (c) no correction. Offset in electron momentum is reasonably small after the $R_{xy}$-dependent $\mathrm{d}E/\mathrm{d}x$ correction by this study. The middle and right plots in Fig. 7 show photon energy difference between measurement and MC generation in various regions of $R_{xy}$ and $\cos\theta_{e^\pm}$. Here, $\theta_{e^\pm}$ is the polar angle of electron momentum. It is seen that the bias in photon energy after the $\mathrm{d}E/\mathrm{d}x$ correction by this study becomes much smaller. Notice that the radiative length of materials for the beam pipe, the VC and the MDC used in $\mathrm{d}E/\mathrm{d}x$ correction is quoted from Ref. [5].

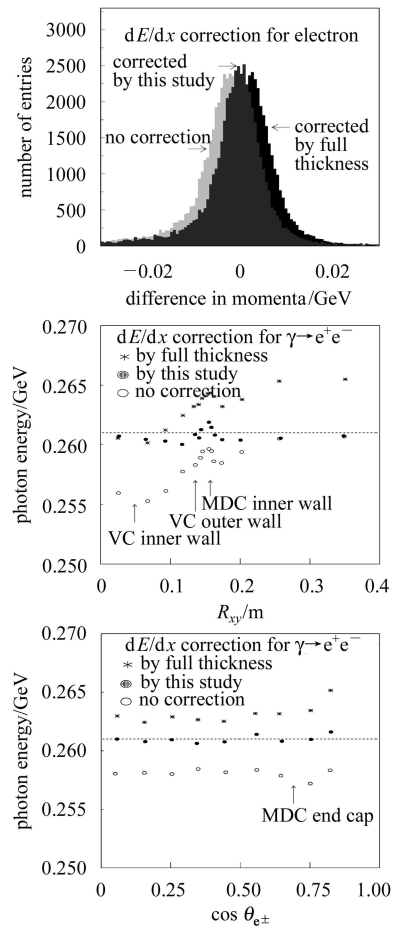


Fig. 7. Momentum difference of the electrons between measurement and MC generation (upper). Photon energy versus $R_{xy}$ (middle) and $\cos\theta_{e^\pm}$ (down). Three cases: $\mathrm{d}E/\mathrm{d}x$ corrections are made by this study, full thickness of materials in the beam-pipe region and no correction.

## 5 Energy scale for photon

Momentum of charged particles at BESⅡ has been well calibrated[7], and thus measured masses for the $K^0_S$, $K^{*0}(892)$ and $\phi$ resonances are in good agreement with the PDG's values[6]. Momentum of daughter particles from decays of these resonances is higher, while that for electrons from photon conversions is usually much lower and even reaches a marginal limit in momentum measurement. Hence, it is necessary to check the lower momentum scale, as well as the energy scale of the photons reconstructed from $e^+e^-$ pairs.

Large amount of $\pi^0$ mesons can be found in the $J/\psi$ decays. A data sample of $\pi^0$ mesons decaying to two photons, with both converted to $e^+e^-$ pair, are selected from the $58\times10^6$ $J/\psi$ events. To suppress hadron contamination, electron identification is applied. Good photons are selected with the same selection criteria as described in the previous section. Background is further suppressed by requiring $E_\gamma \leqslant$ 1GeV for both photons and $0.75 < |\cos\theta_{\gamma\gamma}| < 0.97$, where $\theta_{\gamma\gamma}$ is the opening angle between two photons.

Selections of $\pi^0\to\gamma\gamma$ with both photons in conversion to $e^+e^-$ pair from the $J/\psi$ data yields $503\pm 66$ $\pi^0$s. A MC sample of $63\times10^6$ $\pi^0$s is generated with the same momentum and polar angular distributions as that found from the $\pi^0$ data sample. The invariant mass distributions of $\gamma\gamma$ pairs selected from the $J/\psi$ data and the MC $\pi^0$ sample, after the specific $dE/dx$ correction for the electrons, are fitted to an improved CB function plus a 1st order polynomial background (see Fig. 8). The resulting $\pi^0$ mass, $(134.47\pm0.42)\text{MeV}/c^2$ in the data and $(134.86\pm0.20)\text{MeV}/c^2$ in the MC, are consistent with the PDG's value of $134.98\text{MeV}/c^2$ within error.

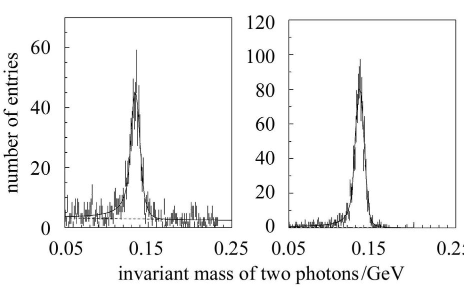


Fig. 8.　Fitting of invariant mass of photon pair from the $J/\psi$ data (left) and MC (right). The solid line is the fit.

Furthermore, large statistics of two photon events produced in the QED process of $e^+e^-\to\gamma\gamma$ may provide precise test in high energy region. The $J/\psi\to\gamma\gamma$ decay is a C-violating process, and thus its contamination in selecting two photon samples is negligible. A MC sample using QED radiative two photon generator (radgg)[3] is generated, and events with one photon converted to $e^+e^-$ pair are selected. Two photons are required to be emitted in back-to-back directions. The fitted photon energies, $(1547.68\pm0.77)$MeV in data and $(1548.73\pm0.39)$MeV in MC, agree with each other within an error at the same level as that for the correction factor of the magnetic field[7]. Our study assures that the energy scale of photons reconstructed from $e^+e^-$ pair is correct in the energy region from 100 to 1550MeV.

## 6　Energy resolution function for photon

Electrons traversing detector may lose energy via the processes of bremsstrahlung and ionization[6]. The bremstrahlung induces a long tail at the lower side of electron energy distribution, and thus the energy loss caused by it is hard to be corrected. For the case of small thickness of material in the BES beam pipe region and electron energy above a few tens of MeV, the energy loss for electrons in the central part of the energy distribution is dominated by the ionization of atoms. Multiple scattering of electrons, specially at large angle, may bring additional tail effect at both the lower and upper sides in the photon energy distribution. The ionization loss of electrons in the detector can be corrected with the effective materials traversed. However, the uncertainty in determining the photon conversion point may bring an additional error to the corrected photon energy at the conversion point.

Overall detector resolution in photon energy measurement using photon conversion technology can be well modeled by full MC simulation. Under an assumption of pure E1 transition, the polar angle distributions for photon productions in the $\psi(2S)\to\gamma\chi_{cJ}$ decays ($J$=0,1,2) have a form of $1+k\cos^2\theta$[8], where the coefficient $k=1$, $-\dfrac{1}{3}$ and $\dfrac{1}{13}$ for $\chi_{c0}$, $\chi_{c1}$ and $\chi_{c2}$, respectively. A MC sample of $5\times10^7$ photons from the $\psi(2S)\to\gamma\chi_{cJ}$ decays with the corresponding polar angle distributions are generated.

The original Crystal Ball (CB) function, $f_{CB}(x)$, has a Gaussian in the central and upper regions but a long tail at the lower side[9].

$$f_{\mathrm{CB}}(x)=\begin{cases} S\cdot\left(\dfrac{n_1}{a_1}\right)^{n_1}\cdot\mathrm{e}^{-\frac{a_1^2}{2}}\cdot\left(\dfrac{n_1}{a_1}+\dfrac{E_0-a_1\sigma-x}{\sigma}\right)^{-n_1} \\ \qquad\qquad \text{if } x\leqslant E_0-a_1\sigma, \\ S\cdot\mathrm{e}^{-\frac{1}{2}(\frac{x-E_0}{\sigma})^2} \qquad \text{if } x\geqslant E_0-a_1\sigma. \end{cases}$$

Our study shows that the CB function does not fit the energy distribution at its upper side in photon conversions. The shape of energy spread for signal photons reconstructed from the converted $\mathrm{e}^+\mathrm{e}^-$ pairs in full region can be well fitted by an Improved Crystal Ball (ICB) function, $f_{\mathrm{ICB}}(x)$, which is defined as the same as the CB except an additional tail at the upper side.

$$f_{\mathrm{ICB}}(x)=\begin{cases} S\cdot\left(\dfrac{n_1}{a_1}\right)^{n_1}\cdot\mathrm{e}^{-\frac{a_1^2}{2}}\cdot\left(\dfrac{n_1}{a_1}+\dfrac{E_0-a_1\sigma-x}{\sigma}\right)^{-n_1} \\ \qquad\qquad \text{if } x\leqslant E_0-a_1\sigma, \\ S\cdot\mathrm{e}^{-\frac{1}{2}(\frac{x-E_0}{\sigma})^2} \quad \text{if } E_0+a_2\sigma\geqslant x\geqslant E_0-a_1\sigma, \\ S\cdot\left(\dfrac{n_2}{a_2}\right)^{n_2}\cdot\mathrm{e}^{-\frac{a_2^2}{2}}\cdot\left(\dfrac{n_2}{a_2}-\dfrac{E_0+a_2\sigma-x}{\sigma}\right)^{-n_2} \\ \qquad\qquad \text{if } x\geqslant E_0+a_2\sigma, \end{cases}$$

where $x$ is the observed photon energy. There are seven parameters: mean and resolution of photon energy ($E_0$, $\sigma$), tail shape at the lower and upper sides ($n_1$, $a_1$) and ($n_2$, $a_2$), and normalization factor $S$.

If we take widths of both $\psi(2S)$ and $\chi_{\mathrm{cJ}}$ states to be zero and mass to be values given by the PDG[6], then photons produced from the $\psi(2S)\to\gamma\chi_{\mathrm{cJ}}$ decays would carry monochromatic energy of 260.72, 171.27 and 127.50MeV for the $\chi_{\mathrm{cJ}}$ ($J=0,1,2$) final states, respectively. The observed energy distributions of the signal photons from the $\psi(2S)\to\gamma\chi_{\mathrm{cJ}}$ decays in MC are given in Fig. 9.

Fits of the photon energy distributions to the ICB function are performed, and the fitting results for photon energy and detector resolution are shown in Fig. 9 and Table 2. The deviations in the resulting photon energy from the input values in the MC are negligibly small for the $\chi_{\mathrm{c0}}$ and $\chi_{\mathrm{c1}}$ states, while that for the $\chi_{\mathrm{c2}}$ state is as large as 0.24±0.06MeV. The latter is attributed to the uncertainty in the $\mathrm{d}E/\mathrm{d}x$ correction for the very low momentum electron. Three sets of ICB parameters for the $\psi(2S)\to\gamma\chi_{\mathrm{cJ}}$ ($J=0,1,2$) decays are listed in Table 3, which can be fed back as input data to a detector resolution function for the $\chi_{\mathrm{cJ}}$ widths measurement[2].

Table 2. Fitted results for photon energy and its resolution from the $\psi(2S)\to\gamma\chi_{\mathrm{cJ}}$ ($J=0,1,2$) decays. The ICB function is used in the fit.

| state | $\chi_{\mathrm{c0}}$ | $\chi_{\mathrm{c1}}$ | $\chi_{\mathrm{c2}}$ |
|---|---|---|---|
| $E_\gamma$/MeV input | 260.72 | 171.27 | 127.50 |
| $E_\gamma$/MeV output | 260.74±0.03 | 171.32±0.03 | 127.74±0.06 |
| $\sigma_{E_\gamma}$/MeV output | 3.78±0.04 | 2.58±0.04 | 2.26±0.11 |

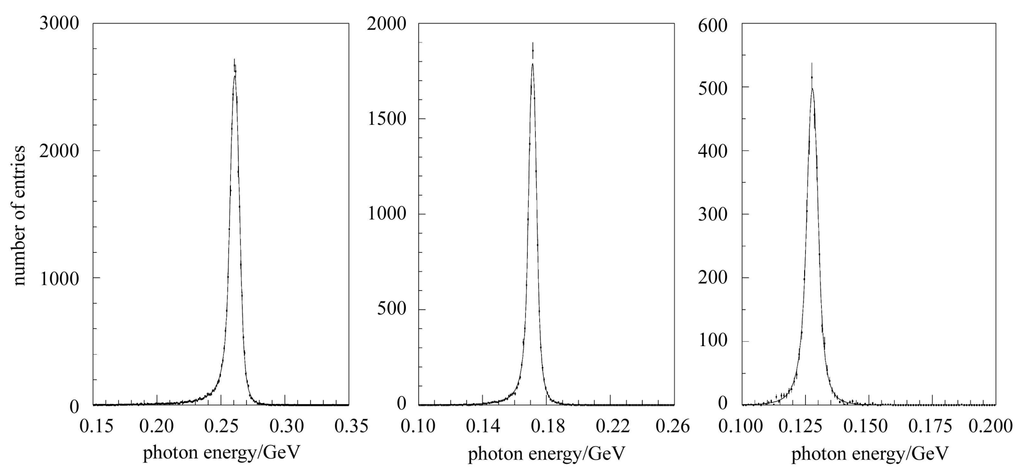


Fig. 9. Energy spectrum of signal photons from the $\psi(2S)\to\gamma\chi_{\mathrm{cJ}}$ decays with zero widths of both $\psi(2S)$ and $\chi_{\mathrm{cJ}}$ for the $\chi_{\mathrm{c0}}$(left), $\chi_{\mathrm{c1}}$(mid) and $\chi_{\mathrm{c2}}$(right) final states. The points are the MC. The solid line are the fit to the ICB function.

Table 3. The parameters of the ICB function for photons from the $\psi(2S) \to \gamma\chi_{cJ}$ ($J = 0,1,2$) decays.

| state | $\chi_{c0}$ | $\chi_{c1}$ | $\chi_{c2}$ |
|---|---|---|---|
| $\sigma$/MeV | 3.78074 | 2.57692 | 2.26002 |
| $\alpha_1$ | 1.3265 | 1.3019 | 1.1416 |
| $N_1$ | 1.9839 | 2.3521 | 4.5556 |
| $\alpha_2$ | 1.6128 | 1.4119 | 1.2900 |
| $N_2$ | 5.7821 | 4.6773 | 4.8321 |

## 7 Energy dependence for detection efficiency and resolution

Energy dependence for the photon detection efficiency and energy resolution is studied in a photon energy region from 100 to 400MeV using MC method. Totally $10^8$ of monochromatic photons at different energy points with polar angle distributions, as the same as that for the $\psi(2S) \to \gamma\chi_{cJ}$ and $\chi_{cJ} \to$ anything decays, are generated. The observed photon energy distributions at each energy point are fitted to the ICB function. The efficiency is calculated as a ratio of signal yield over a number of MC generated events. It includes the effects of detector geometry, MDC tracking, photon reconstruction, angular distribution of photon production, and photon conversion rate. The resulting curves for photon detection efficiency and energy resolution as a function of photon energy are shown in Fig. 10. Three curves in each plot correspond to different polar angle distributions for the $\chi_{cJ}$ ($J=0,1,2$) states.

Further study shows that the detection efficiency calculated by using the $\psi(2S)\to\gamma\chi_{cJ}$ and $\chi_{cJ} \to$ anything MC events, is notably lower than that from the MC events where charged tracks from the $\chi_{cJ}$ decays are removed. It means that the increased multiplicity of charged tracks in MC events causes lower efficiency of track reconstruction for low momentum electrons. The energy resolution is 2.3MeV for 100MeV energy photon, and increased to be 5.5MeV for 400MeV energy photon.

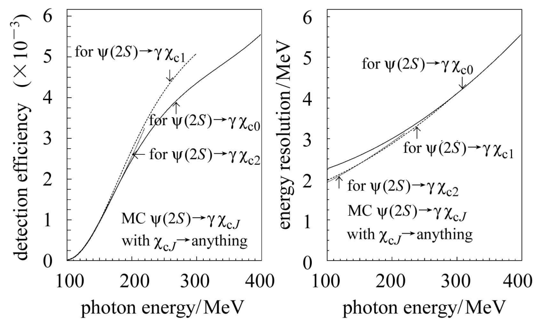


Fig. 10. Photon detection efficiency (left) and energy resolution (right) as a function of photon energy. Here photons have the polar angle distributions as that required for the $\psi(2S) \to \gamma\chi_{cJ}$ ($J=0,1,2$) and $\chi_{cJ} \to$ anything (Lund_crm) decays.

## 8 Conclusion

We have employed the photon conversion technique in photon energy measurement. Using Monte Carlo technique, reconstruction of photon conversions is studied, and the photon detection efficiency and energy resolution as a function of photon energy are obtained. The d$E$/d$x$ correction for the electrons and the energy scale for the photons are calibrated with the BESⅡ data. Our study shows that the energy distribution of the photons can be well fitted to the ICB function. Photon energy resolutions in the range from 2.3 to 3.8MeV for the BESⅡ detector are found for the photons with the energy from 100 to 260MeV, and it provides a tool to measure the $\chi_{cJ}$ ($J=0,1,2$) states precisely from the $\psi(2S)$ radiative decays [2]. Measurement of low energy photons using photon conversions may benefit from the improved energy resolution, better ratio of signal over noise and more precise energy scale, relative to that using CSI calorimeter, and thus the method is expected to have its application in specific physics topic at high luminosity experiment in future.

*We would like to thank C.Z. Yuan and J.C. Chen for their experience in MC simulation.*

## References

1 Athar S B et al(CLEO Collab.). Phys. Rev., 2004, **D70**: 112002

2 Ablikim M et al(BES Collab.). Phys. Rev., 2005, **D71**: 092002

3 Ablikim M et al(BES Collab.). Nucl. Instrum. and Methods, 2005, **A552**: 344

4 BAI J Z et al(BES Collab.). Nucl. Instrum. and Methods, 1994, **A344**: 319; Nucl. Instrum. Methods, 2001, **A458**: 627

5 HONG T et al. HEP & NP, 2001, **25**: 607 (in Chinese) (洪涛等. 高能物理与核物理, 2001, **25**: 607)

6 Eidelman S et al(Particle Data Group). Phys. Lett., 2004, **B592**: 1

7 A Correction Factor $s = 0.9975 \pm 0.0007$ for Magnetic Field at the BESⅡ is Determined with Mass Measurement of the J/ψ Reconstructed from $\psi(2S) \rightarrow \pi^{+}\pi^{-}J/\psi$ and $J/\psi \rightarrow \mu^{+}\mu^{-}$ Decays.

8 Karl G, Meshkov S, Rosner J L. Phys. Rev., 1976, **D13**: 1203; LIU Feng. PhD thesis, ψ′ Hadronic Decays Involving ω and φ, and Polarization of $\psi' \rightarrow \chi_c$ Decays. IHEP, Academy of Chinese Sciences, Beijing, April 2000

9 Brock I C. A Fitting and Plotting Package Using MINUIT, Version 4.07. Dec. 22th, 2000


# 北京谱仪上光子转换过程的重建与光子能量的精确测量*


张长春[1,2;1)] 王喆[3] 袁野[1]

1 (中国科学院高能物理研究所 北京 100049)

2 (北京大学技术物理系 北京 100871)

3 (清华大学工程物理系 北京 100084)



**摘要** 利用蒙特卡罗模拟方法, 研究了光子转换过程的重建, 并得到了依赖于光子能量的光子探测效率及其能量分辨的函数分布. 电子的能量损失校正与光子的能量标度均用北京谱仪的真实数据做了刻度. 研究表明, 改进的晶体球(CB)函数能较好地描述由电子对重建出的光子能量分布. 在北京谱仪实验上, 对于100—260MeV能量的光子, 由电子对转换方法测量的光子能量分辨可达到2.3—3.8MeV.



**关键词** 光子转换 光子重建 d$E$/d$x$能损的校正 光子能量分辨 BESⅡ探测器



2005 – 09 – 09 收稿, 2005 – 12 – 29 收修改稿

*国家自然科学基金(19991480)和中国科学院知识创新工程项目(U-503(高能所))资助



1) E-mail: zhangcc@ihep.ac.cn